

# The modified Cassie's equation and contact angle hysteresis

Xianmin Xu · Xiaoping Wang

Received: 20 July 2012 / Accepted: 27 July 2012  
© Springer-Verlag 2012

**Abstract** In this paper, we derive a modified Cassie's equation for wetting on chemically patterned surfaces from a homogenization approach. The derivation reveals that effective contact angle is a local average of the static contact angle along the contact line which describes all possible equilibrium states including the local minimum of the free energy of the system. The usual Cassie's state which corresponds to the global minimum is only a special case. We then discuss the contact angle hysteresis on chemically patterned surfaces.

**Keywords** The Cassie's equation · Wetting hysteresis · Homogenization

---

This article is part of the Topical Collection on *Contact Angle Hysteresis*

---

This publication was based on work supported in part by Award No SA-C0040/UK-C0016, made by King Abdullah University of Science and Technology (KAUST), Hong Kong RGC-CERG grants 603107 and 604209, Chinese NSFC project 11001260, and by National Center for Mathematics and Interdisciplinary Sciences, CAS.

---

X. Xu (✉)  
The State Key Laboratory of Scientific and Engineering Computing, Institute of Computational Mathematics and Scientific/Engineering Computing, Chinese Academy of Sciences, Beijing 100080, China  
e-mail: xmxu@lsec.cc.ac.cn

X. Wang  
Department of Mathematics, The Hong Kong University of Science and Technology, Clear Water Bay, Kowloon, Hong Kong, China  
e-mail: mawang@ust.hk

## Introduction

The study of wetting phenomenon is of critical importance for many industrial applications [2, 9, 10]. Wetting is the ability of a liquid to maintain contact with a solid surface. In physics, the phenomenon is characterized by two well-known equations, the Young–Laplace equation and the Young equation. The Young–Laplace equation,

$$p_L - p_G = 2\gamma_{LG}\kappa, \quad (1)$$

relates the mean curvature of the interface by the capillary pressure difference across the interface. The Young equation [23],

$$\gamma_{LG} \cos \theta_Y = \gamma_{SG} - \gamma_{SL}, \quad (2)$$

on the other hand, relates the static contact angle to the surface tensions between the three phases: solid, liquid, and gas. In Eqs. 1 and 2,  $p_L$  and  $p_G$  denote the pressures in liquid and gas respectively.  $\kappa$  is the mean curvature of the interface.  $\gamma_{LG}$ ,  $\gamma_{SG}$ , and  $\gamma_{SL}$  denote the liquid–gas surface tension, the solid–gas, and solid–liquid surface tensions, respectively.  $\theta_Y$  is the microscopic contact angle between the liquid–gas interface and the solid surfaces. The angle  $\theta_Y$  is generally called Young's angle.

The behavior of the droplet on rough or chemically inhomogeneous surface are more complicated. In these cases, the actual effective contact angle  $\theta_a$  is generally not equal to the Young's angle  $\theta_Y$  given by Eq. 2. Instead, there are two other equations describing the

relations between  $\theta_a$  and  $\theta_Y$ . One is the so-called the Wenzel's equation [18] for rough surface cases:

$$\cos \theta_a = R \cos \theta_Y, \quad (3)$$

with  $R$  being the ratio of the rough solid surface area and the effective smooth surface area. The other is the Cassie's equation [4] for chemically patterned surfaces (composed by two materials):

$$\cos \theta_a = \rho \theta_{Y1} + (1 - \rho) \theta_{Y2}, \quad (4)$$

where  $\theta_{Y1}$  and  $\theta_{Y2}$  are the Young's angle of the two materials, and  $\rho$  is the area fraction of material 1.

The validity of the Wenzel's equation and Cassie's equation has been investigated for many years (see [1, 3, 20, 21] among many others). There are still many controversies on the two equations [7, 8, 12, 13, 15]. The complexity of the problem also comes from the contact angle hysteresis (CAH). The effective contact angle of liquid drops on rough or inhomogeneous surfaces could take a range of values, depending on the history of the liquid drop. It is believed that the multiple effective contact angles are related to the local minimums of the free energy of the system, which cannot be described by Eqs. 3 or 4. Among those possible effective angles, the largest one is called the advancing angle and the smallest is called the receding angle, and the difference between the advancing and receding angle is called contact angle hysteresis. There have been intensive studies on CAH see [11, 16, 17, 19, 22] among many others, although the theory on CAH is still very incomplete.

In this paper, we derive a modified Cassie's equation for chemically rough surfaces from the Young–Laplace equation and the Young equation. The behavior of the solution for a periodically patterned surface is studied in the limit of the small  $\varepsilon$  period. The results show that effective contact angle is a local average of the static contact angle along the contact line which describes all possible equilibrium states including the local minimum of the free energy of the system. The usual Cassie's state which corresponds to the global minimum is only a special case. We illustrate the results by several examples. Combine with our results on CAH for two-dimensional results in [22], we also characterize CAH on some chemically patterned surfaces.

The paper is organized as follows: In section “Derivation of the modified Cassie's equation”, we introduce a simple model and derive the effective contact angle from a homogenization approach. The meaning of the rough parameter is then explained by some examples. In section “The contact angle hysteresis

on chemically patterned surface”, we discuss CAH on chemically patterned surfaces.

## Derivation of the modified Cassie's equation

### A simple model

We first consider a simple case shown in Fig. 1. A channel is formed by two planes parallel to the  $xy$  plane. The bottom of the channel is composed of periodically patterned two materials, static contact angles  $\theta_{Y1}$  and  $\theta_{Y2}$ , respectively. We assume that the liquid–gas interface is almost planar except near the rough bottom surface. The top of the channel has a variable equilibrium contact angle so that it has no affect on the contact angle on the bottom (similar models have been used in some recent numerical and molecular dynamics simulations [6, 14]). We assume the pattern is periodic in both  $x$  and  $y$  with period  $\varepsilon$  and contact angle function

$$\theta_Y(x, y) = \begin{cases} \theta_{Y1}, & \text{if } (x, y) \text{ is in material 1;} \\ \theta_{Y2}, & \text{if } (x, y) \text{ is in material 2.} \end{cases} \quad (5)$$

### The Young–Laplace equation and the modified Cassie's equation

For the above system, we may assume the liquid–gas interface is given by

$$x = f(y, z) = kz + \varepsilon u\left(\frac{y}{\varepsilon}, \frac{z}{\varepsilon}\right). \quad (6)$$

Here,  $k$  is a constant, and  $\varepsilon$  is the period of the pattern along  $y$ -axis. Introduce the fast variables  $Y = \frac{y}{\varepsilon}$  and  $Z = \frac{z}{\varepsilon}$ . We suppose  $u(Y, Z)$  is a smooth function periodic in  $Y$  with period 1 and such that  $\lim_{Z \rightarrow \infty} u(Y, Z) = 0$  and  $\lim_{Z \rightarrow \infty} \nabla u(Y, Z) = 0$ . Equation 6 represents an interface which differs from the plane  $x = kz$  only near the bottom surface  $z = 0$ . In  $\varepsilon \rightarrow 0$  limit, the effective contact angle is then the

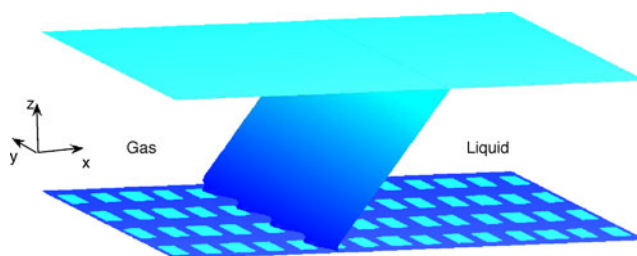


**Fig. 1** The channel

angle between the plane  $x = kz$  and the bottom  $z = 0$ , as shown in Fig. 2a, given by

$$\cos \theta_a = \frac{k}{1 + k^2}. \tag{7}$$

In addition, as shown in Fig. 2b, we can also compute the unit normal of the interface  $x = f(y, z) = kz + \varepsilon u(\frac{y}{\varepsilon}, \frac{z}{\varepsilon})$  pointing to the liquid domain,

$$\begin{aligned} \mathbf{n} &= \frac{1}{\sqrt{1 + (\partial_y f)^2 + (\partial_z f)^2}} \begin{pmatrix} 1 \\ -\partial_y f \\ -\partial_z f \end{pmatrix} \\ &= \frac{1}{\sqrt{1 + (\partial_Y u)^2 + (k + \partial_Z u)^2}} \begin{pmatrix} 1 \\ -\partial_Y u \\ -(k + \partial_Z u) \end{pmatrix}. \end{aligned}$$

Notice that the mean curvature of the interface is given by  $\kappa = \nabla \cdot \mathbf{n}$  with  $\nabla = (\partial_x, \partial_y, \partial_z)^T$ . By direct computation, we have

$$\kappa = \varepsilon \tilde{\nabla} \cdot \left[ \frac{1}{\sqrt{1 + (\partial_Y u)^2 + (k + \partial_Z u)^2}} \begin{pmatrix} \partial_Y u \\ k + \partial_Z u \end{pmatrix} \right],$$

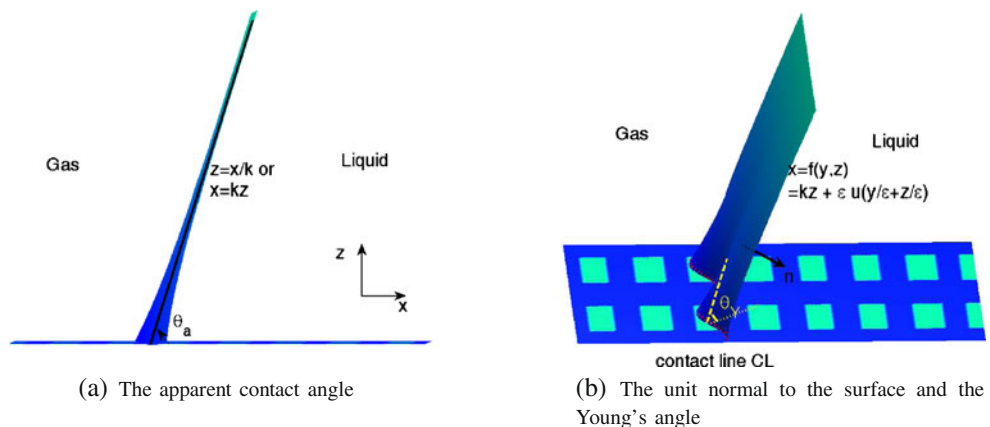
with  $\tilde{\nabla} = (\partial_Y, \partial_Z)^T$ . The Young–Laplace Eq. 1, assuming equal pressure across the interface, is then given by

$$\tilde{\nabla} \cdot \left[ \frac{1}{\sqrt{1 + (\partial_Y u)^2 + (k + \partial_Z u)^2}} \begin{pmatrix} \partial_Y u \\ k + \partial_Z u \end{pmatrix} \right] = 0. \tag{8}$$

The contact line  $CL$  between the interface  $x = kz + \varepsilon u(\frac{y}{\varepsilon}, \frac{z}{\varepsilon})$  and the solid boundary  $z = 0$  (see Fig. 2b) is now given by

$$\begin{cases} x = \varepsilon u(y/\varepsilon, 0), \\ z = 0. \end{cases}$$

**Fig. 2** Geometry properties of the liquid–gas interface



The local contact angle at the contact line is given by

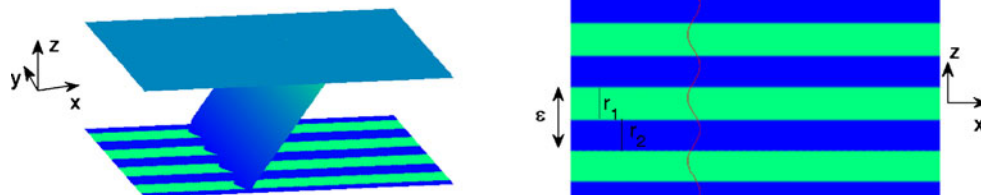
$$\begin{aligned} \cos \theta_Y \left( \frac{x}{\varepsilon}, \frac{y}{\varepsilon} \right) |_{(x,y) \in CL} &= \cos \theta_Y \left( u \left( \frac{y}{\varepsilon}, 0 \right), \frac{y}{\varepsilon} \right) \\ &= \cos \theta_Y (u(Y, 0), Y) = -\mathbf{n}|_{CL} \cdot \mathbf{e}_3 \\ &= \frac{k + \partial_Z u(Y, 0)}{\sqrt{1 + (\partial_Y u(Y, 0))^2 + (k + \partial_Z u(Y, 0))^2}}. \end{aligned} \tag{9}$$

Here,  $\mathbf{e}_3 = (0, 0, 1)^T$  is the basis along  $z$  direction. Given a patterned surface defined by Eq. 5, we can assume that the interface is a small perturbation of a plane. The next order perturbation  $u(Y, Z)$  is then determined by Eq. 8 with the boundary condition 9 and a decay condition for  $Z \rightarrow \infty$ .

Integrating Eq. 8 in the domain of fast parameter  $\{(Y, Z) \mid 0 < Y < 1, 0 < Z < \infty\}$  and using the boundary condition 9 and the decaying property as  $Z \rightarrow \infty$ , we have

$$\begin{aligned} 0 &= \int_0^\infty \int_0^1 \tilde{\nabla} \cdot \left[ \frac{1}{\sqrt{1 + (\partial_Y u)^2 + (k + \partial_Z u)^2}} \begin{pmatrix} \partial_Y u \\ k + \partial_Z u \end{pmatrix} \right] dY dZ \\ &= \lim_{Z_0 \rightarrow \infty} \int_0^1 \frac{k + \partial_Z u}{\sqrt{1 + (\partial_Y u)^2 + (k + \partial_Z u)^2}} \Big|_{Z=Z_0} dY \\ &\quad + \int_0^1 \frac{-(k + \partial_Z u)}{\sqrt{1 + (\partial_Y u)^2 + (k + \partial_Z u)^2}} \Big|_{Z=0} dY \\ &\quad + \int_0^\infty \frac{\partial_Y u}{\sqrt{1 + (\partial_Y u)^2 + (k + \partial_Z u)^2}} \Big|_{Y=1} dZ \\ &\quad + \int_0^\infty \frac{-\partial_Y u}{\sqrt{1 + (\partial_Y u)^2 + (k + \partial_Z u)^2}} \Big|_{Y=0} dZ \\ &= \frac{k}{\sqrt{1 + k^2}} - \int_0^1 \frac{(k + \partial_Z u)}{\sqrt{1 + (\partial_Y u)^2 + (k + \partial_Z u)^2}} \Big|_{Z=0} dY \\ &= \cos \theta_a - \int_0^1 \cos \theta_Y (u(Y, 0), Y) dY. \end{aligned}$$

**Fig. 3** The case of  $x$ -directional striped bottom surface



Therefore, we have the effective contact angle

$$\cos \theta_a = \int_0^1 \cos \theta_Y(u(Y, 0), Y) dY. \quad (10)$$

In original variables of  $x$ ,  $y$ , and  $z$ , the equation reads

$$\cos \theta_a = \frac{1}{\varepsilon} \int_0^\varepsilon \cos \theta_Y(x, y) \Big|_{x=eu(\frac{y}{\varepsilon}, 0)} dy. \quad (11)$$

The righthand side term is the integral average of the local static contact angle along the contact line in one period of  $y$ . We call Eqs. 10 or 11 the modified Cassie's equation. It provides an explicit formula to compute the effective contact angle once we know the patterns of the solid surface and the contact line location which can be solved from Eqs. 8 and 9.

A few examples

To understand the meaning of the Eq. 11, we firstly consider two special cases with striped bottom surfaces (see Figs. 3 and 4). We suppose that the two materials on the bottom have different contact angle  $\theta_{Y1}$  and  $\theta_{Y2}$ . For the first case (Fig. 3), the stripes lie along the  $x$  direction and the contact line goes across all the stripes. From Eq. 11, it is easy to see that the effective contact angle  $\theta_a$  is given by

$$\cos \theta_a = \lambda \cos \theta_{Y1} + (1 - \lambda) \cos \theta_{Y2},$$

with  $\lambda = \frac{r_1}{\varepsilon}$  which is also consistent with Eq. 4. As shown in Fig. 3, here  $r_1$  is the width of material 1 strip

and  $\varepsilon$  is the sum of the width of material 1 strip and that of material 2 strip in one period. The effective contact angle is independent of the position and the shape of the contact line. The  $\lambda$  is also the area fraction of material 1 in the bottom surface in the special case. For the second case (Fig. 4), the stripes lie along the  $y$  direction and  $u(Y, Z)$  is independent of  $Y$ . From the Eq. 11, the effective contact angle  $\theta_a$  is either

$$\theta_a = \theta_{Y1}$$

when the contact line locates in material 1, or

$$\theta_a = \theta_{Y2}$$

when the contact line locates in material 2. The result is consistent with our analysis in [22]. In this case, the effective contact angle could not be described by the usual Cassie's Eq. 4, where the area fraction is used as a roughness parameter.

From the above two examples, we see that the area fraction of the chemically patterned surface, by itself, cannot determine the effective contact angle. Instead, it can be accurately described by Eq. 11. In this sense, the effective contact angle is determined only by the material properties along the contact line. The location and the shape of the contact line is determined by the function  $u(Y, Z)$  which can be solved from Eqs. 8 and 9.

We now consider examples with more complicated rough structures. For simplicity, we draw only the bottom surface and some possible locations of the contact

**Fig. 4** The case of  $y$ -directional striped bottom surface



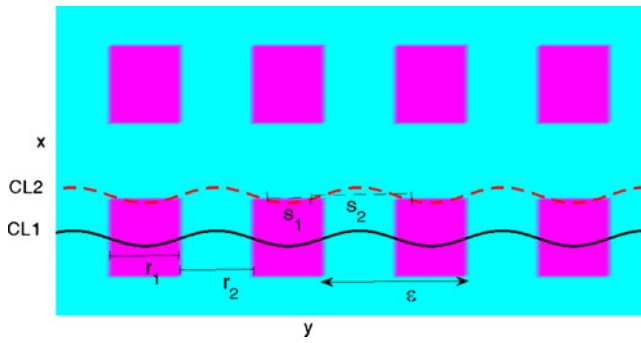


**Fig. 5** The chemically patterned bottom surface and two contact lines

line. One example is a chemically patterned surface in two directions (see Fig. 5 and notice that we draw  $y$  axis horizontally). The base material has a contact angle  $\theta_{Y1}$  and the material in the square patch has a contact angle  $\theta_{Y2}$ . We assume two possible contact lines  $CL1$  and  $CL2$  which are both periodic along the  $y$  direction, but at different locations.

According to the Eq. 11, the effective contact angles corresponding the  $CL1$  and  $CL2$  are respectively given by

$$\cos \theta_{a,i} = \lambda_i \cos \theta_{Y1} + (1 - \lambda_i) \cos \theta_{Y2}, \tag{12}$$

with  $\lambda_1 = \frac{r_1}{\epsilon}$  and  $\lambda_2 = \frac{s_1}{\epsilon}$ . Here,  $r_1$  and  $s_1$  are respectively the distances of the contact line  $CL1$  and  $CL2$  across material 1 in one period. The Eq. 12 has a similar form to the original Cassie's Eq. 4. However, the parameter  $\lambda_i$  in the equation is a length fraction of the material along the contact line. It is quite different from the parameter in Eq. 4, which is an area fraction of the material.

The problem can be generalized to patterns with more than two materials. We consider a solid surface

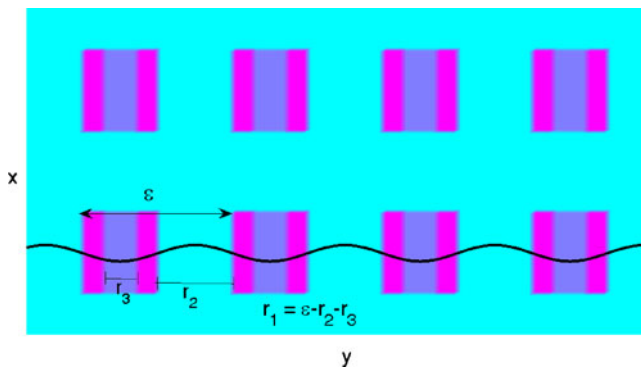


**Fig. 6** The chemically patterned bottom surface with three materials

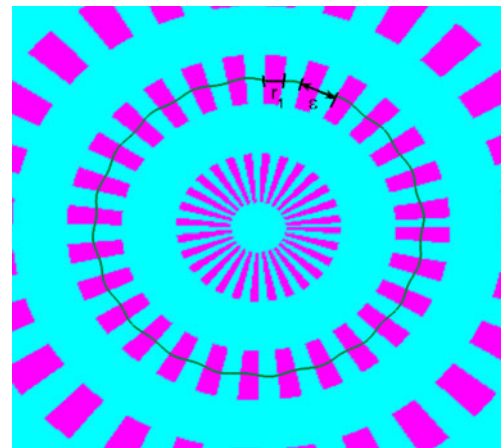


**Fig. 7** The chemically patterned bottom surface with three materials

which is periodically patterned with  $n$  materials with contact angle  $\theta_{Yi} (n > 2)$ , see, for example, Fig. 6. When the period  $\epsilon$  is very small, then the effective contact angle is given by

$$\cos \theta_a = \sum_{i=1}^n \tilde{\lambda}_i \cos \theta_{Yi}, \tag{13}$$

with  $\tilde{\lambda}_i = \frac{r_i}{\epsilon}$  being the length fraction of material  $i$  along the contact line.

Finally, we consider a liquid drop on a radially patterned surface. Here, the contact line is almost a circle as shown in Fig. 7. Assuming the period  $\epsilon$  is relatively small compared to the drop radius, then the effective contact angle is given by, according to the Eq. 12,

$$\cos \theta_a \approx \lambda \cos \theta_{Y1} + (1 - \lambda) \cos \theta_{Y2}, \tag{14}$$

with  $\lambda = \frac{r_1}{\epsilon}$  being the width fraction of material 1 along the contact line (see Fig. 7).

**The contact angle hysteresis on chemically patterned surface**

In section “The CAH on striped surface”, we first review some analytic results on CAH on chemically patterned surfaces for a two-dimension problem. Then, combining the results with the modified Cassie’s equation discussed in section “Derivation of the modified Cassie’s equation”, we study the CAH for 3D wetting

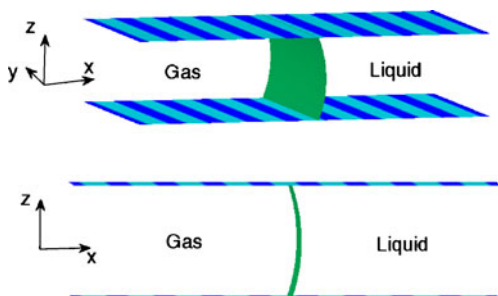


**Fig. 8** The striped patterned channel and the reduced two-dimensional channel

problems in section “Discussions of the CAH for more general cases”.

The CAH on striped surface

We consider a channel composed by two parallel planar surfaces. Both surfaces have the same striped chemically pattern, as shown in Fig. 8. The channel is filled with liquid and gas. In this section, we allow the pressures in liquid and in gas to be different. The three phase contact lines are supposed to be parallel to the strip. In this case, the model is reduced to a two dimensional model as shown in Fig. 8.

We have recently studied this two-dimensional problem in [22]. Suppose the boundary is composed with the two materials  $A$  and  $B$ , with different Young’s angles  $\theta_A$  and  $\theta_B$  ( $\theta_A < \theta_B$ ). Then, the equilibrium con-

tact angle  $\theta_{eq}$  is determined only by the location of the contact point  $\tilde{\mathbf{x}}_0$ . There are only three possible cases (also shown in Fig. 9):

$$\theta_{eq} = \begin{cases} \theta_A, & \text{if } \tilde{\mathbf{x}}_0 \in \mathcal{A}; \\ \theta_B, & \text{if } \tilde{\mathbf{x}}_0 \in \mathcal{B}; \\ \theta_\zeta, & \text{if } \tilde{\mathbf{x}}_0 \in \mathcal{R}; \end{cases} \tag{15}$$

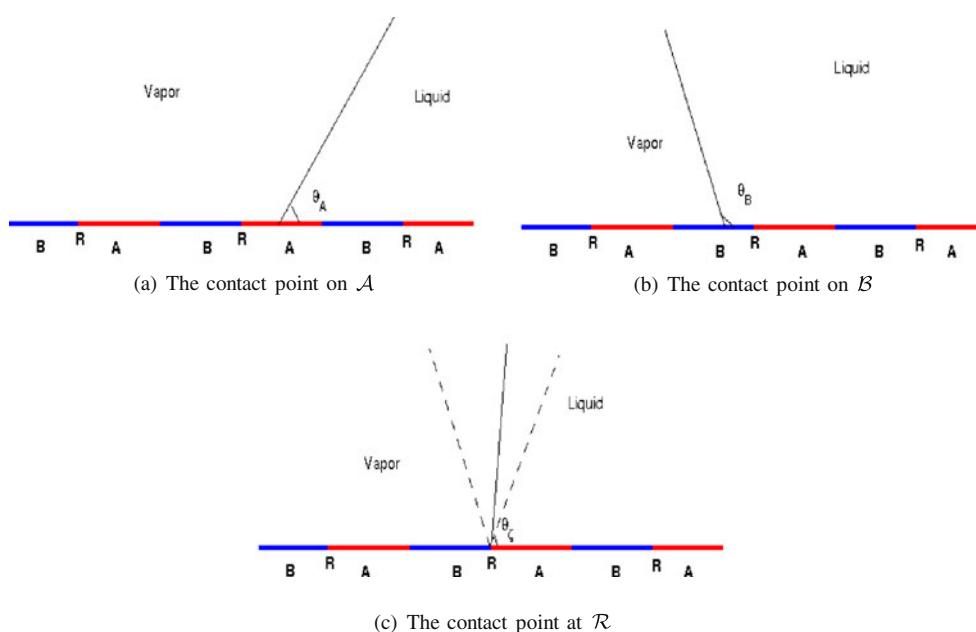
with  $\theta_\zeta$  such that  $\theta_A \leq \theta_\zeta \leq \theta_B$ . On the joint points of the two materials, the value of the contact angle is not unique and has to be determined by additional conditions.

For the above channel model (with  $\theta_A < \theta_B$ ), we considered a quasi-static flow in [22]. When the volume of liquid is gradually increased and decreased, we always consider the local minimizers of the system energy. We find that, when the chemical patterns becomes finer and finer, the advancing contact angle approaches to  $\theta_B$  (the largest Young’s angle on the solid surface) and the receding contact angle approaches to  $\theta_A$  (the smallest Young’s angle on the solid surface). For proof and more explanations of the results, we refer to Section 5 in [22]. We remark that the result is only correct for two-dimensional wetting problems. In the next subsection, we discuss three dimensional situations.

Discussions of the CAH for more general cases

We now consider the contact angle hysteresis for a channel composed by two plans with periodic pattern in

**Fig. 9** The contact angles on chemically patterned surface



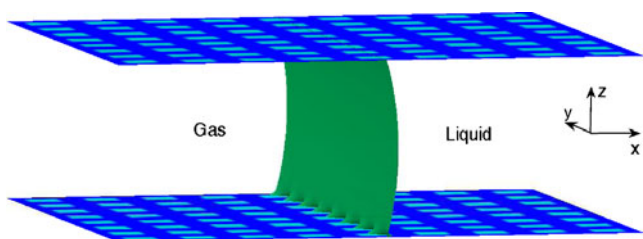


**Fig. 10** The channel with chemically patterned solid boundary

both  $x$  and  $y$  directions, as shown in Fig. 10. The liquid–gas interface is lying (almost) parallel to  $y$  direction. Just as before, we assume that the base material has a contact angle  $\theta_{Y1}$  and the square patch material has a contact angle  $\theta_{Y2}$  with  $\theta_{Y1} < \theta_{Y2}$ .

Again from homogenization (similar to the derivation of the Eq. 12), we have the following conclusion. When the contact line is located in the base region, the effective contact angle is

$$\theta_{a1} = \theta_{Y1}; \tag{16}$$

and when the contact line intersects with the array of the square patch in  $y$  direction (similar to the CL1 in Fig. 5), the effective contact angle is

$$\cos \theta_{a2} = (1 - \lambda) \cos \theta_{Y1} + \lambda \cos \theta_{Y2}, \tag{17}$$

with  $\lambda$  being the ratio of the square spot width to one period of the pattern in  $y$  direction. When the contact line intersects only partly with the array of the square patch (as CL2 in Fig. 5), the effective contact angle is  $\theta_\zeta$  such that  $\theta_{a1} < \theta_\zeta < \theta_{a2}$ .

The result is similar to the Eq. 15 of the two-dimensional channel in last subsection. Taken the homogenized problem as a two-dimensional model, we can deduce that the advancing contact angle for the channel is  $\theta_{a2}$  (given by the Eq. 16) and the receding contact angle is  $\theta_{a1}$  (given by the Eq. 17).

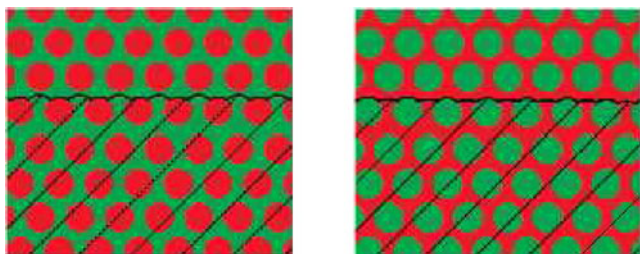


**Fig. 11** Water on two surfaces with 50 % surface area of two components with different contact angles (taken from [8])

At the end of the section, we study an example given in [5, 8]. As shown in Fig. 11, we show two configurations with equal amounts of different surface areas. They contain circular spots of radius  $r$  which are periodically placed with the distance between two nearest spot centers being about  $2.693r$ . The green regions has a smaller contact angle than the red regions. Denote the contact angles for the green area and the red area are  $\theta_{Y1}$  and  $\theta_{Y2}$  ( $\theta_{Y1} < \theta_{Y2}$ ), respectively.

Suppose that the contact line is almost straight as shown in Fig. 11. By the analysis in last section, it is easy to compute the maximum and minimum effective contact angles for the two configurations. For the left one, the minimum effective contact angle, which is also the receding contact angle, is

$$\theta_{rec} = \theta_{Y1};$$

and the maximum effective contact angle, which is also advancing contact angle, is such that

$$\cos \theta_{adv} = \lambda \cos \theta_{Y1} + (1 - \lambda) \cos \theta_{Y2},$$

with  $\lambda = (2.693r - 2r)/(2.693r) \approx 0.257$ . For the right configuration, the receding contact angle is

$$\cos \tilde{\theta}_{rec} = (1 - \lambda) \cos \theta_{Y1} + \lambda \cos \theta_{Y2},$$

and the advancing contact angle is

$$\tilde{\theta}_{adv} = \theta_{Y2}.$$

The two configurations have very different wetting properties, although their area ratio is the same. This is consistent in principle with some existing analytic and experimental results [5, 7, 8].

### Conclusion

From a simple wetting model with chemically patterned surface, we derive, by homogenization, a modified Cassie equation by homogenization which describes the apparent contact angle. We give some examples to show that the effective contact angle is a local average of the static contact angle along the contact line. Combining the modified Cassie equation with some existing results on CAH for the two-dimensional wetting problem in [22], we then discuss CAH for the general three-dimensional wetting phenomena on chemically patterned surfaces with some examples. We show that the modified Cassie equation can be used to describe

CAH while the usual Cassie's state, which only corresponds to the global minimum of the total energy of the system, is unable to explain the CAH phenomena.

## References

- Alberti G, DeSimone A (2005) Wetting of rough surfaces: a homogenization approach. *Proc R Soc A* 451:79–97
- Bonn D, Eggers J, Indekeu J, Meunier J, Rolley E (2009) Wetting and spreading. *Rev Mod Phys* 81:739–805
- Bormashenko E (2009) A variational approach to wetting of composite surfaces: is wetting of composite surfaces a one-dimensional or two-dimensional phenomenon? *Langmuir* 25(18):10451–10454
- Cassie A, Baxter S (1944) Wettability of porous surfaces. *Trans Faraday Soc* 40:546–551
- Chen W, Fadeev AY, Hsieh M, Öner D, Youngblood J, McCarthy TJ (1999) Ultrahydrophobic and ultralyophobic surfaces: some comments and examples. *Langmuir* 15:3395–3399
- Dimitrov DI, Milchev A, Binder K (2010) Method for wettability characterization based on contact line pinning. *Phys Rev E* 81:04163
- Gao L, McCarthy TJ (2007) How Wenzel and Cassie were wrong. *Langmuir* 23:3762–3765
- Gao L, McCarthy TJ (2007) Reply to “Comment on How Wenzel and Cassie were wrong by Gao and McCarthy”. *Langmuir* 23:13243–13243
- de Gennes PG (1985) Wetting: statics and dynamics. *Rev Mod Phys* 57:827–863
- de Gennes PG, Brochard-Wyart F, Quere D (2003) *Capillarity and wetting phenomena*. Springer, Berlin
- Johnson RE Jr, Dettre RH (1964) Contact angle hysteresis. III. Study of an idealized heterogeneous surfaces. *J Phys Chem* 68:1744–1750
- Marmur A, Bittoun E (2009) When Wenzel and Cassie are right: reconciling local and global considerations. *Langmuir* 25:1277–1281
- Mchale G (2007) Cassie and Wenzel: were they really so wrong. *Langmuir* 23:8200–8205
- Mognetti BM, Yeomans JM (2009) Modeling receding contact lines on superhydrophobic surfaces. *Langmuir* 26:18162–18168
- Panchagnula MV, Vedantam S (2007) Comment on how Wenzel and Cassie were wrong by Gao and McCarthy. *Langmuir* 23:13242–13242
- Schwartz LW, Garoff S (1985) Contact angle hysteresis on heterogeneous surfaces. *Langmuir* 1:219–230
- Turco A, Alouges F, DeSimone A (2009) Wetting on rough surfaces and contact angle hysteresis: numerical experiments based on a phase field model. *M2AN* 43:1027–1044
- Wenzel RN (1936) Resistance of solid surfaces to wetting by water. *Ind Eng Chem* 28:988–994
- Whyman G, Bormashenko E, Stein T (2008) The rigorous derivative of Young, Cassie–Baxter and Wenzel equations and the analysis of the contact angle hysteresis phenomenon. *Chem Phys Lett* 450:355–359
- Wolansky G, Marmur A (1999) Apparent contact angles on rough surfaces: the Wenzel equation revisited. *Colloids Surf A* 156:381–388
- Xu X, Wang X-P (2010) Derivation of Wenzel's and Cassie's equations from a phase field model for two phase flow on rough surface. *SIAM J Appl Math* 70:2929–2941
- Xu X, Wang X-P (2011) Analysis of wetting and contact angle hysteresis on chemically patterned surfaces. *SIAM J Appl Math* 71:1753–1779
- Young T (1805) An essay on the cohesion of fluids. *Philos Trans R Soc Lond* 95:6587